

Article

An Enzyme- and Label-Free Fluorescence Aptasensor for Detection of Thrombin Based on Graphene Oxide and G-Quadruplex

Yani Wei ¹, Luhui Wang ¹, Yingying Zhang ² and Yafei Dong ^{1,2,*}

¹ College of Life Sciences, Shaanxi Normal University, Xi'an 710119, China; weiyani@snnu.edu.cn (Y.W.); wangluhui@snnu.edu.cn (L.W.)

² School of Computer Science, Shaanxi Normal University, Xi'an 710119, China; zhangyingying@snnu.edu.cn

* Correspondence: dongyf@snnu.edu.cn

Received: 9 September 2019; Accepted: 10 October 2019; Published: 12 October 2019



Abstract: An enzyme- and label-free aptamer-based assay is described for the determination of thrombin. A DNA strand (S) consisting of two parts was designed, where the first (Sa) is the thrombin-binding aptamer and the second (Se) is a G-quadruplex. In the absence of thrombin, Sa is readily adsorbed by graphene oxide (GO), which has a preference for ss-DNA rather than for ds-DNA. Upon the addition of the N-methyl-mesoporphyrin IX (NMM), its fluorescence (with excitation/emission at 399/610 nm) is quenched by GO. In contrast, in the presence of thrombin, the aptamer will bind thrombin, and thus, be separated from GO. As a result, fluorescence will be enhanced. The increase is linear in the 0.37 nM to 50 μ M thrombin concentration range, and the detection limit is 0.37 nM. The method is highly selective over other proteins, cost-effective, and simple. In our perception, it represents a universal detection scheme that may be applied to other targets according to the proper choice of the aptamer sequence and formation of a suitable aptamer-target pair.

Keywords: thrombin detection; fluorescence; aptamer; N-methyl-mesoporphyrin IX (NMM)

1. Introduction

In the fields of biomedicine and biotechnology, it is essential to detect bioactive molecules with high sensitivity and selectivity. Therefore, the emergence of biosensors has provided a convenient and fast method for concentration determinations of biomolecules, such as proteins, genes, and ions. In past research, antibody-linked immunosorbent assays (ELISA) have been widely used to detect proteins [1,2]. However, the approach is expensive and takes a lot of time to complete, as it requires incubation and multi-step washing processes [3,4]. Aptamers are single-stranded nucleic acids, i.e., DNA or RNA, which may be selected from random sequence nucleic acid libraries by an in vitro selection process named SELEX (Systematic Evolution of Ligands by Exponential Enrichment) [5,6]. Compared with antibodies, aptamers have many advantages, such as simple modification, easy production, chemical stability and reusability, easy storage, and low cost [7–12]. Aptamers have great binding affinity and high specificity for a variety of targets, for example, small molecules, proteins, metal ions, or cell surfaces [13–15]. Therefore, aptamers are considered to be the promising candidate for the construction of sensors, including electrochemical sensors, fluorescence aptasensors, and colorimetric sensors [13,16,17].

Recently, fluorescent methods have attracted extensive attention in the field of sensing devices based on aptamers thanks to their high sensitivity and simple operation. According to previous strategies, we have observed that most aptasensors have been designed based on fluorophores and quenchers [18–20]. However, the modification of aptamers is expensive, time-consuming, and requires

complex processes. In addition, modifications with fluorophores and quenchers affect sensitivity due to the weak interaction between aptamers and the corresponding targets [21]. Therefore, taking these constraints into account, a label-free method needs to be proposed for fluorescence detection of thrombin.

Thrombin, a multifunctional protease, plays a critical role in biology and pathological processes, such as thrombosis, cardiovascular disease, and early diagnoses and treatment [22]. In addition, thrombin is virtually nonexistent in the blood of healthy people, although low nanomolar concentrations of thrombin can be produced in early hemostatic processes [23]. Furthermore, high picomolar concentrations of thrombin can be detected in the blood of people with coagulation abnormalities, resulting in certain serious diseases, for example, thromboembolic disease and Alzheimer's disease [24–27]. Therefore, given the great importance of detecting the concentration of thrombin in blood, it is necessary to propose an approach with excellent selectivity and specificity. In prior studies, many approaches have been developed, such as label-free detection [28,29], fluorescence detection [13,28–35], etc. These methods are simple and easy to undertake, and have attracted considerable attention. Some researchers have introduced protease into the detection system, which is sensitive to the reaction conditions [27], and the modification of the aptamer undoubtedly affects the binding ability of the aptamer to the corresponding target [36]. As far as these methods are concerned, they are complicated and expensive. Overall, our method, an enzyme-free, non-label, universal fluorescence aptasensor is more capable of meeting the needs for the detection of thrombin and other targets.

As a new type of nanomaterial, graphene oxide (GO), comprises a single layer of carbon atoms in a densely-packed, honeycomb, two-dimensional lattice [37,38]. GO has many excellent properties, including good water dispersibility [36], high mechanical strength [39,40], etc. GO has a unique adsorption capacity, which can selectively absorb ss-DNA by π - π accumulation, instead of ds-DNA or G-quadruplex [41,42]. At the same time, GO can quench the fluorescence of dyes labeled with ss-DNA through the Förster resonance energy transfer (FRET) process [43]. Up to now, GO has been widely used to construct biosensors thanks to these excellent properties [44–50]. Nanomaterials have been applied to the recognition mechanisms of biomolecules, which has given rise to potential applications in the fields of biomolecular detection systems [51,52]. In addition, as a special deoxyribonucleotide structure, G-quadruplex has also been introduced into our detection system. It is a G-rich fragment that has a significant fluorescent signal after interaction with NMM [50,53]. G-quadruplex overcomes the shortcomings of expensive DNA modification. There is no doubt that G-quadruplex is the promising candidate as a new signal reporter. So far, G-quadruplex has attracted considerable attention in the construction of biosensors and molecular detection [54–58].

Here, through the combination of an advanced nanomaterial (GO) with a special deoxyribonucleotide structure (G-quadruplex), we constructed an enzyme-free, label-free, and simple approach for sensitive fluorescent detection of thrombin. In the presence of thrombin, we obtained high fluorescence upon the formation of a duplex of the target/aptamer. This enzyme- and label-free method can successfully detect thrombin, which makes it simple to use, time-saving, and cost-effective. This method provides a universal platform which can detect targets specifically according to the specific binding of the aptamer to its target.

2. Experimental Section

2.1. Materials and Reagents

DNA oligonucleotides were purchased from Shanghai Sangon Biotechnology Co (Shanghai, China); their sequences are listed in Table 1. Thrombin was derived from bovine plasma (lyophilized powder, 40–300 NIH units/mg protein). Lysozyme, thrombin, IgG, human serum albumin (HSA), and bovine serum albumin (BSA) were purchased from Sigma (St. Louis, MO, USA). Trypsin was purchased from Shanghai Sangon Biotechnology Co. (Shanghai, China). N-methylmesoporphyrin IX

(NMM) was purchased from J&K Scientific Ltd. (Beijing, China). The stock solution of NMM was diluted with dimethyl sulfoxide (DMSO) and stored at $-20\text{ }^{\circ}\text{C}$. Graphene Oxide (GO) was purchased from Nanjing XFNANO Materials Tech Co., Ltd (Nanjing, China) and suspended in water via sonication. All other materials were purchased from Xi'an JingBo Bio-Technique Co. (Xi'an, China). The fetal bovine serum samples were obtained from the Lanzhou Roya Bio-Technology Co. (Lanzhou, China), Ltd, and diluted with a reaction buffer 100 times before use.

Table 1. Sequences of oligonucleotides.

Name	Sequences (5'-3')
S	AGTCCGTGGTAGGGCAGGTTGGGGTGACTGGGTAGGGCGGGTTGGG
S1	AGTCCGTGGTAGGGCAGGTTGGGGTGACTGGGTA
S2	AGTCCGTGGTAGGGCAGGTTGGGGTGACTGGGTAGGGC
S3	AGTCCGTGGTAGGGCAGGTTGGGGTGACTGGGTAGGGCGGGT

The underlined letters, S, S1, S2, S3, are the sequences of G-quadruplex; others refer to the thrombin aptamer sequence.

2.2. Apparatus

Fluorescence emission spectra were measured using an EnSpire ELIASA from PerkinElmer (Waltham, MA, USA). The fluorescence spectra of NMM was excited at 399 nm and emitted at 610 nm. A fluorescence intensity at 608 nm was used to evaluate the performance of the experiments.

2.3. The Sensing Procedure

First, thrombin, S ($0.25\text{ }\mu\text{M}$) and the buffer (20 mM Tris-HCl, 100 mM NaCl, 10 mM KCl, 10 mM MgCl_2 , pH = 7.5) were mixed for 30 min at $37\text{ }^{\circ}\text{C}$. Then, GO ($30\text{ }\mu\text{g}\cdot\text{mL}^{-1}$) was added into the reaction system and mixed for 30 min at room temperature. Next, NMM ($1.5\text{ }\mu\text{M}$) was added to the final reaction samples, and the fluorescence intensity was measured after mixing for 25 min at $37\text{ }^{\circ}\text{C}$. Finally, we recorded the fluorescence spectra.

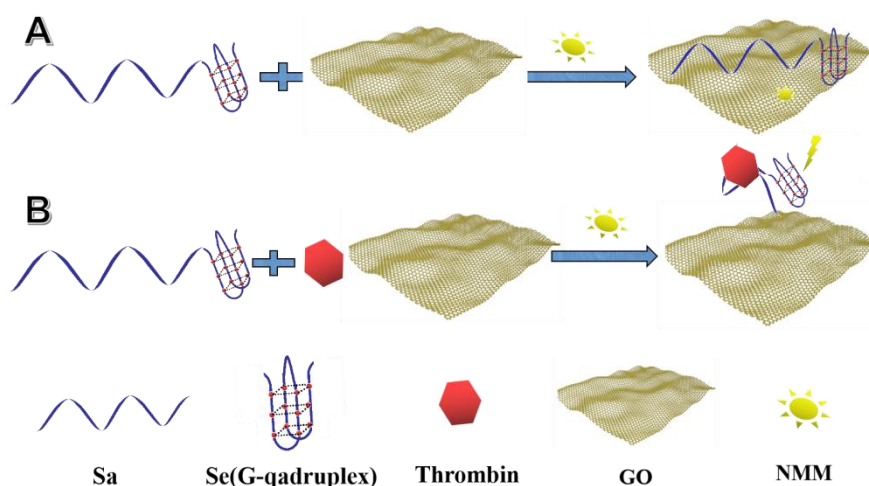
2.4. Selectivity of the Thrombin Assay

S ($0.25\text{ }\mu\text{M}$) was mixed with thrombin ($0.2\text{ }\mu\text{M}$) or other non-specific proteins (Lysozyme, Trypsase, IgG, BSA and HSA $2\text{ }\mu\text{M}$) respectively. Subsequent operations were consistent with the process described above.

3. Results and Discussion

3.1. Principle of the Method

The proposed method for label-free and enzyme-free thrombin detection based on GO and G-quadruplex is illustrated in Scheme 1. The well-designed DNA strand S was introduced into the system, which consisted of two parts: Sa is the thrombin aptamer sequence, and Se is the sequence of the G-quadruplex. First, S bound to the surface of the GO through π - π stacking; in the presence of thrombin, it binds to the Se part (aptamer sequence) due to the high binding affinity between the target and the corresponding aptamer. The ss-DNA could be anchored to the surface of the GO; the Se/Thrombin duplex would then strip the G-quadruplex from the GO. After that, in the final stage, NMM was inserted into the G-quadruplex and used to emit a high fluorescence. In the absence of thrombin, S was still anchored to the GO surface, resulting in a low fluorescence intensity. Consequently, thrombin could be detected simply and with sensitivity by observing the fluorescence intensity change of NMM. The proposed method could be used for the detection of other targets by changing the corresponding aptamer.



Scheme 1. Schematic illustration of the universal, no-label, enzyme-free fluorescent detection of thrombin-based on graphene oxide and G-quadruplex.

3.2. The Feasibility of the Strategy

We check the feasibility of thrombin detection by recording the fluorescence intensities under different conditions. As shown in Figure 1, only if the NMM was added individually could a weak fluorescence of NMM (curve e, green curve) be obtained. However, a significant fluorescence intensity enhancement (curve b, red curve) was recorded because of the interaction between the G-quadruplex and NMM. However, in the coexistence of S and GO, the system showed a low fluorescence of NMM after the incubation of S with GO for 30 min (curve d, purple curve), due to the absorption function between GO and ss-DNA(S). The fluorescent signal was regarded as a background signal, which proved the high quenching ability of GO. In contrast, when thrombin was present, the hybridization between thrombin and its aptamer promoted the formation of a duplex of thrombin/Sa, which liberated the S form GO and notably increased the NMM fluorescence (curve c, blue curve) compared with the curve d (in the absence of a target). These results confirm the feasibility of the proposed biosensor.

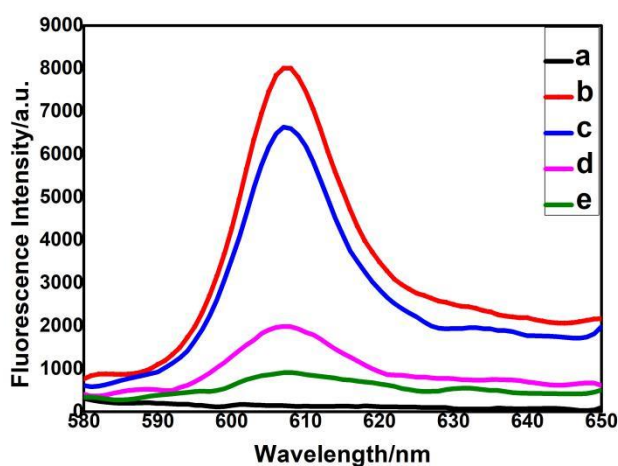


Figure 1. Fluorescence-emission spectra of the different samples: (a) S; (b) S + NMM; (c) S + Thrombin + GO + NMM; (d) S + GO + NMM; (e) NMM. The concentrations of S, thrombin, GO, and NMM are 0.25 μM , 0.2 μM , 30 $\mu\text{g}\cdot\text{mL}^{-1}$, and 1.5 μM , respectively.

3.3. Optimization of Experimental Conditions

To achieve the best performance, we optimized the various experimental conditions, including the concentration of S, the concentration of GO, the reaction time between the G-quadruplex and NMM,

and the length of terminal signal carrier sequence. F and F_0 denote the fluorescence intensity of NMM in the presence and absence of thrombin. F_0 is regarded as a blank group.

In the method, G-quadruplex is the terminal signal carrier and has a potentially significant effect on the intensity of the fluorescence. The long length of the G-quadruplex had a weak interaction with GO, resulting in a high quenching efficiency and low background signal. As shown in Figure 2A, F/F_0 is increased as the length of G-quadruplex is increased (from one-quarter complete to complete G-quadruplex). Finally, F/F_0 reached a peak when the length of the G-quadruplex was 17-mer.

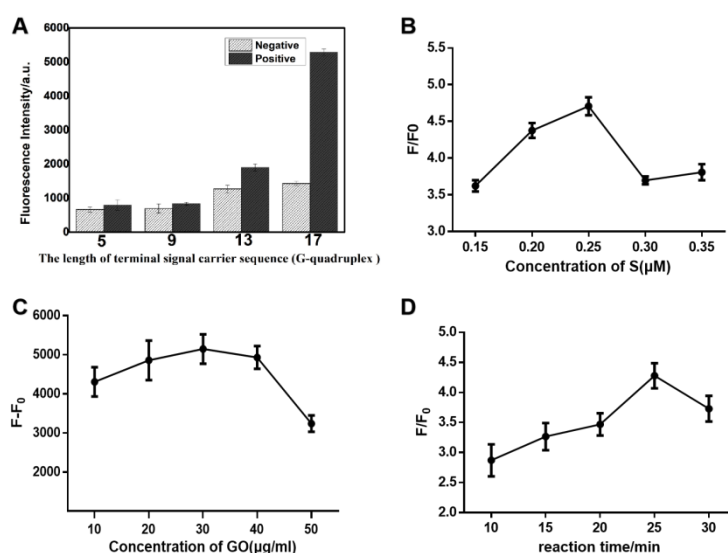


Figure 2. (A) Effect of the length of the terminal signal carrier sequence (G-quadruplex) upon fluorescence emission spectra; (B) Effect of the concentration of S upon fluorescence emission spectra; (C) Effect of the concentration of GO upon fluorescence emission spectra; (D) Effect of the reaction time between G-quadruplex structure and NMM upon fluorescence emission spectra. The error bar was calculated in three independent experiments.

As shown in Figure 2B, the initial fluorescence was low with lower concentrations of S, and the change in the intensity of the fluorescence was not obvious. However, the system presented the opposite results with higher concentrations. The F/F_0 gradually increased to a range of 0.15 μM to 0.25 μM , and reached a maximum at 0.25 μM , before subsequently decreasing. Therefore, due to its optimal signal-to-noise level, the best concentration of S was found to be 0.25 μM in follow-up experiments. According to Figure 2C, the ΔF value gradually increased with increasing the GO concentration in the range from 10 $\mu\text{g}\cdot\text{mL}^{-1}$ to 30 $\mu\text{g}\cdot\text{mL}^{-1}$, before gradually decrease thereafter. The mixed solution containing a low concentration of GO resulted in a high background signal; however, a high concentration of GO led to fluorescence quenching of the duplex of S/Thrombin/NMM. Furthermore, 30 $\mu\text{g}\cdot\text{mL}^{-1}$ was selected to achieve a better signal. In addition, the fluorescence intensity was also influenced by the interaction time between the G-quadruplex and NMM. As shown in Figure 2D, F/F_0 has a high ratio of signal-to-noise (SNR), reaching a maximum at 25 min.

3.4. Analytical Performance

The evaluation criteria of the analytical performance are sensitive and play an important role in accurate detections. Based on optimized conditions, we evaluated the sensitivity by varying the concentration of thrombin. Figure 3A shows that a gradual increase in the fluorescence signal was attained as the concentration of thrombin increased from 0 μM to 50 μM . The fluorescence intensity at 608 nm is linear to the concentration of thrombin; the calibration plot obtained is shown in Figure 3B. The linear regression equation can be described as follows: $Y = 1900.5 \times \text{Log}_{10}\text{Concentration} + 1467.6$, with a good correlation coefficient of 0.9947. According to the 3 σ rule (3 σ /S, in which σ is the standard

deviation for the blank solution and S is the slope of the linear equation), the limit of this detection method for thrombin is estimated to be 0.37 nM. Compared to other methods, the method proposed in the paper has a low detection limit (Table 2). More importantly, it is simple, due to its enzyme- and label-free design.

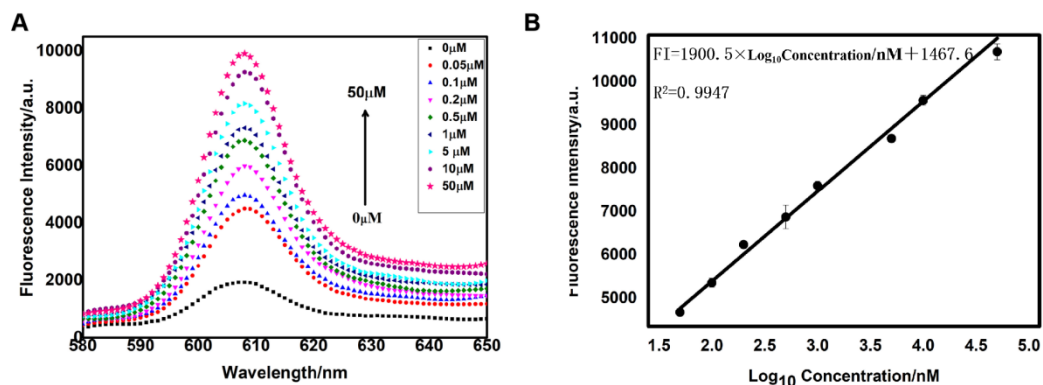


Figure 3. (A) Fluorescence emission spectra of the sensing method to different concentrations of thrombin. From a to i, the concentration of thrombin is 0, 0.05, 0.1, 0.2, 0.5, 1, 5, 10, 50 μM , respectively; (B) The linear region from 0.05 μM to 50 μM of thrombin, yielding a detection limit of 0.37 nM. The error bar was calculated in three independent experiments.

Table 2. Comparison of the methods with a recently published investigation for thrombin.

Methods	Analytical Range	Detection Limit (nM)	Ref.
Fluorescence detection	1.1–500 nM	1.1	[13]
Fluorescence detection	0.59–35 nM	0.59	[33]
Fluorescence detection	0.7 nM–0.16 μM	0.7	[34]
Fluorescence detection	2.21–25 nM	2.21	[35]
Fluorescence detection	0.37 nM–50 μM	0.37	This work

3.5. Selectivity of Thrombin Detection

The specificity of the method was investigated with different, nonspecific proteins, including lysozyme, trypsin, IgG, human serum albumin (HSA), and bovine serum albumin (BSA) at a concentration of 2 μM to study the selectivity. As shown in Figure 4, the detection system emitted a weak fluorescence response to the nonspecific proteins. However, due to the specificity of the aptamer to its target, in the presence of thrombin, enhanced fluorescence of NMM was observed in comparison to other circumstances. These data demonstrate the excellent selectivity of the fluorescent aptasensor; it can be regarded as a specific and selective platform for target protein detection.

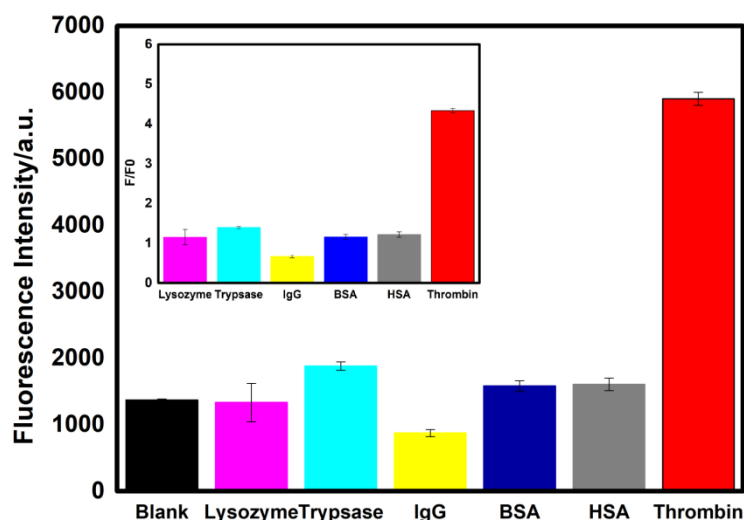


Figure 4. Selectivity evaluation of the biosensor for the detection of thrombin against other proteins of Lysozyme, Trypsase, IgG, BSA, and HSA. The concentration of the thrombin was 0.2 μM . However, the concentration of Lysozyme, Trypsase, IgG, BSA, and HSA was 2 μM . No thrombin or other proteins were used in the blank group. Inset: the changes in fluorescence intensity (F/F_0), F and F_0 , are the fluorescence intensities in the presence and absence of protein, respectively. The error bar was calculated in three independent experiments.

3.6. Determination of Thrombin in Actual Samples (Serum)

In order to verify the feasibility of the assay in real samples. Experiments were carried out by adding different concentrations of thrombin to bovine serum. A significantly enhanced fluorescence signal could be observed in both the buffer and serum compared with the blank control (Figure 5). In addition, we measured the recovery; the range was shown to be 97%–110% (Table 3). Overall, the results show the excellent applicability of the proposed method for thrombin detection in real samples.

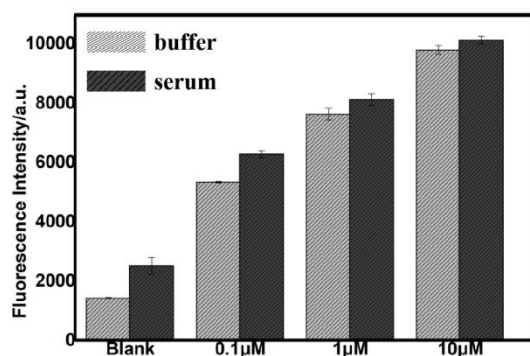


Figure 5. Results obtained from the fluorescent tests of diluted serum samples spiked with different concentrations of thrombin and thrombin in buffer. The same reaction mixtures without thrombin were used as the blank group. The error bar was calculated from three independent experiments.

Table 3. Recovery tests in actual samples.

Samples	Thrombin Added	Detected	SD	Recovery
1	0.1 μM	0.11 μM	30.8%	110%
2	1 μM	0.97 μM	21.7%	97%
3	10 μM	10.65 μM	19.6%	106.5%

4. Conclusions

In summary, this paper proposes a non-label and enzyme-free fluorescence aptasensor based on graphene oxide and G-quadruplex for thrombin detection. In our work, the aptamer could bind to its target, and thus, be separated from GO. After adding NMM, it emitted strong fluorescence. Additionally, the system showed excellent selectivity in the detection of other proteins. Our methodology has several distinct advantages. First, an aptamer probe without any label is involved, which is critical for retaining the excellent binding activity between the target and its aptamer, and makes the process cost effective, time-saving, and simple. Second, the feasibility and applicability of the mechanism were verified theoretically and empirically. Third, as a new type of nanomaterial, GO is easy to prepare in large quantities; it is a cost-effective and universal platform which can meet the needs of future practical applications. Moreover, our platform can be applied to the detection of other targets by changing the aptamers to form a suitable aptamer-target pair. Other molecules also can be detected, such as acetamiprid, cocaine, etc. In other words, our assay has potential applications in the fields of biology, biomedicine, biochemistry, and so on.

Author Contributions: Y.W. and L.W. proposed and designed models; Y.W. performed the experiments, data analysis; Y.Z. and Y.D. commented and upgraded the manuscript.

Funding: This work was supported by National Natural Science Foundation of China (Grant No.61572302, No. 61272246), the Shaanxi Normal University Graduate Innovation Fund Project (Supported by the Fundamental Research Funds for the Central Universities, No. 2018CSLY018).

Conflicts of Interest: The authors declare no conflict of interest.

References

1. Lequin, R.M. Enzyme Immunoassay (EIA)/Enzyme-Linked Immunosorbent Assay (ELISA). *Clin. Chem.* **2005**, *51*, 2415–2418. [[CrossRef](#)]
2. Lam, M.T.; Wan, Q.H.; Boulet, C.A.; Le, X.C. Competitive immunoassay for staphylococcal enterotoxin a using capillary electrophoresis with laser-induced fluorescence detection. *J. Chromatogr. A* **1999**, *853*, 545–553. [[CrossRef](#)]
3. Baker, K.N.; Rendall, M.H.; Patel, A.; Boyd, P.; James, D.C. Rapid monitoring of recombinant protein products: A comparison of current technologies. *Trends Biotechnol.* **2002**, *20*, 149–156. [[CrossRef](#)]
4. Stoltenburg, R.; Reinemann, C.; Strehlitz, B. Selex—A (r)evolutionary method to generate high-affinity nucleic acid ligands. *Biomol. Eng.* **2007**, *24*, 381–403. [[CrossRef](#)] [[PubMed](#)]
5. Birch, C.M.; Hou, H.W.; Han, J.; Niles, J.C. Identification of malaria parasite-infected red blood cell surface aptamers by inertial microfluidic SELEX (I-SELEX). *Sci. Rep.* **2015**, *5*, 11347. [[CrossRef](#)] [[PubMed](#)]
6. Cho, E.J.; Lee, J.W.; Ellington, A.D. Applications of aptamers as sensors. *Annu. Rev. Anal. Chem.* **2009**, *2*, 241–264. [[CrossRef](#)] [[PubMed](#)]
7. Tombelli, S.; Minunni, A.A. Analytical applications of aptamers. *Biosens. Bioelectron.* **2005**, *20*, 2424–2434. [[CrossRef](#)] [[PubMed](#)]
8. Shamah, S.M.; Healy, J.M.; Cload, S.T. Complex target selex. *Acc. Chem. Res.* **2008**, *41*, 130–138. [[CrossRef](#)] [[PubMed](#)]
9. Liu, J.; Cao, Z.; Lu, Y. Functional nucleic acid sensors. *Chem. Rev.* **2009**, *109*, 1948. [[CrossRef](#)] [[PubMed](#)]
10. Huang, Y.; Chen, J.; Zhao, S.; Shi, M.; Chen, Z.F.; Liang, H. Label-free colorimetric aptasensor based on nicking enzyme assisted signal amplification and dnzyme amplification for highly sensitive detection of protein. *Anal. Chem.* **2013**, *85*, 4423–4430. [[CrossRef](#)]
11. He, F.; Tang, Y.; Wang, S.; Li, Y.; Zhu, D. Fluorescent amplifying recognition for DNA G-quadruplex folding with a cationic conjugated polymer: A platform for homogeneous potassium detection. *J. Am. Chem. Soc.* **2005**, *127*, 12343–12346. [[CrossRef](#)] [[PubMed](#)]
12. Wang, L.; Liu, X.; Hu, X.; Song, S.; Fan, C. Unmodified gold nanoparticles as a colorimetric probe for potassium DNA aptamers. *Chem. Commun.* **2006**, *36*, 3780–3782. [[CrossRef](#)] [[PubMed](#)]

13. Kong, L.; Xu, J.; Xu, Y.; Xiang, Y.; Yuan, R.; Chai, Y. A universal and label-free aptasensor for fluorescent detection of ATP and thrombin based on SYBR Green I dye. *Biosens. Bioelectron.* **2013**, *42*, 193–197. [[CrossRef](#)] [[PubMed](#)]
14. Xu, Y.; Xu, J.; Xiang, Y.; Yuan, R.; Chai, Y. Target-induced structure switching of hairpin aptamers for label-free and sensitive fluorescent detection of ATP via exonuclease-catalyzed target recycling amplification. *Biosens. Bioelectron.* **2014**, *51*, 293–296. [[CrossRef](#)] [[PubMed](#)]
15. Michaud, M.; Jourdan, E.; Villet, A.; Ravel, A.; Catherine Grosset, A.; Peyrin, E. A DNA aptamer as a new target-specific chiral selector for HPLC. *J. Am. Chem. Soc.* **2003**, *125*, 8672–8679. [[CrossRef](#)] [[PubMed](#)]
16. Fang, X.; Tan, W. Aptamers Generated from Cell-SELEX for Molecular Medicine: A Chemical Biology Approach. *Acc. Chem. Res.* **2010**, *43*, 48–57. [[CrossRef](#)] [[PubMed](#)]
17. Jiang, B.; Wang, M.; Chen, Y.; Xie, J.; Xiang, Y. Highly sensitive electrochemical detection of cocaine on graphene/AuNP modified electrode via catalytic redox-recycling amplification. *Biosens. Bioelectron.* **2012**, *32*, 305–308. [[CrossRef](#)]
18. Zhu, X.; Zhao, J.; Wu, Y.; Shen, Z.; Li, G. Fabrication of a Highly Sensitive Aptasensor for Potassium with a Nicking Endonuclease-Assisted Signal Amplification Strategy. *Anal. Chem.* **2011**, *83*, 4085–4089. [[CrossRef](#)]
19. Zhou, W.; Gong, X.; Xiang, Y.; Yuan, R.; Chai, Y. Target-Triggered Quadratic Amplification for Label-Free and Sensitive Visual Detection of Cytokines Based on Hairpin Aptamer DNAzyme Probes. *Anal. Chem.* **2014**, *86*, 953–958. [[CrossRef](#)]
20. Yang, R.; Tang, Z.; Yan, J.; Kang, H.; Kim, Y.; Zhu, Z. Noncovalent assembly of carbon nanotubes and single-stranded DNA: An effective sensing platform for probing biomolecular interactions. *Anal. Chem.* **2008**, *80*, 7408–7413. [[CrossRef](#)]
21. Stojanovic, M.N.; Prada, P.D.; Landry, D.W. Fluorescent Sensors Based on Aptamer Self-Assembly. *J. Am. Chem. Soc.* **2000**, *122*, 11547–11548. [[CrossRef](#)] [[PubMed](#)]
22. Tang, Z.; Mallikaratchy, P.; Yang, R.; Kim, Y.; Zhu, Z.; Wang, H. Aptamer Switch Probe Based on Intramolecular Displacement. *J. Am. Chem. Soc.* **2008**, *130*, 11268–11269. [[CrossRef](#)] [[PubMed](#)]
23. Kim, B.; Hwan, J.I.; Mijeong, K.; Hongku, S.; Young, W.H. Cationic conjugated polyelectrolytes-triggered conformational change of molecular beacon aptamer for highly sensitive and selective potassium ion detection. *J. Am. Chem. Soc.* **2012**, *134*, 3133–3138. [[CrossRef](#)] [[PubMed](#)]
24. Zhang, J.; Wang, L.; Zhang, H.; Boey, F.; Song, S.; Fan, C. Aptamer-Based Multicolor Fluorescent Gold Nanoprobes for Multiplex Detection in Homogeneous Solution. *Small* **2010**, *6*, 201–204. [[CrossRef](#)] [[PubMed](#)]
25. Xu, W.; Xue, S.; Yi, H.; Jing, P.; Chai, Y.; Yuan, R. A sensitive electrochemical aptasensor based on the co-catalysis of hemin/G-quadruplex, platinum nanoparticles and flower-like MnO₂ nanosphere functionalized multi-walled carbon nanotubes. *Chem. Commun.* **2015**, *51*, 1472–1474. [[CrossRef](#)] [[PubMed](#)]
26. Xue, L.; Zhou, X.; Xing, D. Sensitive and Homogeneous Protein Detection Based on Target-Triggered Aptamer Hairpin Switch and Nicking Enzyme Assisted Fluorescence Signal Amplification. *Anal. Chem.* **2012**, *84*, 3507–3513. [[CrossRef](#)] [[PubMed](#)]
27. Tuleuova, N.; Jones, C.N.; Yan, J.; Ramanculov, E.; Yokobayashi, Y.; Revzin, A. Development of an Aptamer Beacon for Detection of Interferon-Gamma. *Anal. Chem.* **2010**, *82*, 1851–1857. [[CrossRef](#)] [[PubMed](#)]
28. Wang, H.; Liu, Y.; Liu, C.; Huang, J.; Yang, P.; Liu, B. Microfluidic chip-based aptasensor for amplified electrochemical detection of human thrombin. *Electrochem. Commun.* **2010**, *12*, 258–261. [[CrossRef](#)]
29. Shuman, M.A.; Majerus, P.W. The measurement of thrombin in clotting blood by radioimmunoassay. *J. Clin. Investig.* **1976**, *58*, 1249–1258. [[CrossRef](#)]
30. Tan, Y.; Zhang, X.; Xie, Y.; Zhao, R.; Tan, C.; Jiang, Y. Label-free fluorescent assays based on aptamer-target recognition. *Analyst* **2012**, *137*, 2309–2312. [[CrossRef](#)]
31. Yan, S.; Huang, R.; Zhou, Y.; Zhang, M.; Deng, M.; Wang, X. Aptamer-based turn-on fluorescent four-branched quaternary ammonium pyrazine probe for selective thrombin detection. *Chem. Commun.* **2011**, *47*, 1273–1275. [[CrossRef](#)] [[PubMed](#)]
32. Zheng, A.X.; Wang, J.R.; Li, J.; Song, X.R.; Chen, G.N.; Yang, H.H. Enzyme-free fluorescence aptasensor for amplification detection of human thrombin via target-catalyzed hairpin assembly. *Biosens. Bioelectron.* **2012**, *36*, 217–221. [[CrossRef](#)] [[PubMed](#)]
33. Kuang, L.; Cao, S.P.; Zhang, L.; Li, Q.H.; Liu, Z.C.; Liang, R.P. A novel nanosensor composed of aptamer bio-dots and gold nanoparticles for determination of thrombin with multiple signals. *Biosens. Bioelectron.* **2016**, *85*, 798–806. [[CrossRef](#)] [[PubMed](#)]

34. Wang, W.; Xu, D.D.; Pang, D.W.; Tang, H.W. Fluorescent sensing of thrombin using a magnetic nano-platform with aptamer-target-aptamer sandwich and fluorescent silica nanoprobe. *J. Lumin.* **2017**, *187*, 9–13. [[CrossRef](#)]
35. Wang, J.; Li, B.; Lu, Q.; Li, X.; Weng, C.; Yan, X. A versatile fluorometric aptasensing scheme based on the use of a hybrid material composed of polypyrrole nanoparticles and dna-silver nanoclusters: Application to the determination of adenosine, thrombin, or interferon-gamma. *Microchimica Acta* **2019**, *186*, 356. [[CrossRef](#)] [[PubMed](#)]
36. Niu, S.; Qu, L.; Zhang, Q.; Lin, J. Fluorescence detection of thrombin using autocatalytic strand displacement cycle reaction and a dual-aptamer DNA sandwich assay. *Anal. Biochem.* **2012**, *421*, 362–367. [[CrossRef](#)]
37. Fu, B.; Cao, J.; Jiang, W.; Wang, L. A novel enzyme-free and label-free fluorescence aptasensor for amplified detection of adenosine. *Biosens. Bioelectron.* **2013**, *44*, 52–56. [[CrossRef](#)]
38. Choi, M.S.; Yoon, M.; Baeg, J.O.; Kim, J. Label-free dual assay of DNA sequences and potassium ions using an aptamer probe and a molecular light switch complex. *Chem. Commun.* **2009**, *47*, 7419–7421. [[CrossRef](#)]
39. Novoselov, K.S.; Geim, A.K.; Morozov, S.V. Electric Field Effect in Atomically Thin Carbon Films. *Science* **2004**, *306*, 666–669. [[CrossRef](#)]
40. Li, L.L.; Liu, K.P.; Yang, G.H.; Wang, C.M.; Zhang, J.R.; Zhu, J.J. Fabrication of graphene–quantum dots composites for sensitive electrogenerated chemiluminescence immunosensing. *Adv. Funct. Mater.* **2011**, *21*, 869–878. [[CrossRef](#)]
41. Liu, Z.; Robinson, J.T.; Sun, X.; Dai, H. PEGylated Nano-Graphene Oxide for Delivery of Water Insoluble Cancer Drugs. *J. Am. Chem. Soc.* **2008**, *130*, 10876–10877. [[CrossRef](#)] [[PubMed](#)]
42. Dikin, D.A.; Stankovich, S.; Zimney, E.J.; Piner, R.D.; Ruoff, R.S. Preparation and characterization of graphene oxide paper. *Nature* **2007**, *448*, 457–460. [[CrossRef](#)] [[PubMed](#)]
43. Swathi, R.S.; Sebastian, K.L. Long range resonance energy transfer from a dye molecule to graphene has (distance)⁻⁴ dependence. *J. Chem. Phys.* **2009**, *130*, 086101. [[CrossRef](#)] [[PubMed](#)]
44. Wu, W.; Hu, H.; Li, F.; Wang, L.; Gao, J.; Lu, J. A graphene oxide-based nano-beacon for DNA phosphorylation analysis. *Chem. Commun.* **2011**, *47*, 1201–1203. [[CrossRef](#)] [[PubMed](#)]
45. Tang, L.; Chang, H.; Liu, Y.; Li, J. Duplex DNA/Graphene Oxide Biointerface: From Fundamental Understanding to Specific Enzymatic Effects. *Adv. Funct. Mater.* **2012**, *22*, 3083–3088. [[CrossRef](#)]
46. Chun, H.L.; Li, J.; Mei, H.L.; Yi, W.W.; Huang, H.Y.; Chen, X. Amplified Aptamer-Based Assay through Catalytic Recycling of the Analyte. *Angew. Chem.* **2010**, *49*, 8454–8457.
47. He, S.; Song, B.; Li, D.; Zhu, C.; Qi, W.; Wen, Y. A Graphene Nanoprobe for Rapid, Sensitive, and Multicolor Fluorescent DNA Analysis. *Adv. Funct. Mater.* **2010**, *20*, 453–459. [[CrossRef](#)]
48. Chang, H.; Tang, L.; Wang, Y.; Jiang, J.; Li, J. Graphene fluorescence resonance energy transfer aptasensor for the thrombin detection. *Anal. Chem.* **2010**, *82*, 2341–2346. [[CrossRef](#)]
49. Dong, H.; Gao, W.; Yan, F.; Ji, H.; Ju, H. Fluorescence resonance energy transfer between quantum dots and graphene oxide for sensing biomolecules. *Anal. Chem.* **2010**, *82*, 5511–5517. [[CrossRef](#)]
50. Loh, K.P.; Bao, Q.; Eda, G.; Chhowalla, M. Graphene oxide as a chemically tunable platform for optical applications. *Nat. Chem.* **2010**, *2*, 1015–1024. [[CrossRef](#)]
51. Du, D.; Wang, L.; Shao, Y.; Wang, J.; Engelhard, M.H.; Lin, Y. Functionalized Graphene Oxide as a Nanocarrier in a Multienzyme Labeling Amplification Strategy for Ultrasensitive Electrochemical Immunoassay of Phosphorylated p53 (S392). *Anal. Chem.* **2011**, *83*, 746–752. [[CrossRef](#)] [[PubMed](#)]
52. Cui, L.; Lin, X.; Lin, N. Graphene oxide-protected DNA probes for multiplex microRNA analysis in complex biological samples based on a cyclic enzymatic amplification method. *Chem. Commun.* **2011**, *48*, 194–196. [[CrossRef](#)] [[PubMed](#)]
53. Wang, Y.; Li, Z.; Hu, D.; Lin, C.T.; Lin, Y. Aptamer/Graphene Oxide Nanocomplex for in Situ Molecular Probing in Living Cells. *J. Am. Chem. Soc.* **2010**, *132*, 9274–9276. [[CrossRef](#)] [[PubMed](#)]
54. Li, H.; Ren, J.; Liu, Y.; Wang, E. Application of DNA machine in amplified DNA detection. *Chem. Commun.* **2013**, *50*, 704–706. [[CrossRef](#)] [[PubMed](#)]
55. Wang, K.; Ren, J.; Fan, D.; Liu, Y.; Wang, E. Integration of graphene oxide and DNA as a universal platform for multiple arithmetic logic units. *Chem. Commun.* **2014**, *50*, 14390–14393. [[CrossRef](#)]
56. Lv, L.; Guo, Z.; Wang, J.; Wang, E. G-Quadruplex as Signal Transducer for Biorecognition Events. *Curr. Pharm. Design* **2012**, *18*, 2076–2095. [[CrossRef](#)] [[PubMed](#)]

57. Lu, L.; Wang, W.; Wang, M.; Kang, T.S.; Lu, J.J.; Chen, X.P.; Han, Q.B.; Leung, C.H.; Ma, D.L. A luminescent G-quadruplex-selective iridium (III) complex for the label-free detection of lysozyme. *J. Mater. Chem. B* **2016**, *4*, 2407–2411. [[CrossRef](#)]
58. Lu, L.; Mao, Z.; Kang, T.S.; Leung, C.H.; Ma, D.L. A versatile nanomachine for the sensitive detection of platelet-derived growth factor-BB utilizing a G-quadruplex-selective iridium(III) complex. *Biosens. Bioelectron.* **2016**, *85*, 300–309. [[CrossRef](#)]



© 2019 by the authors. Licensee MDPI, Basel, Switzerland. This article is an open access article distributed under the terms and conditions of the Creative Commons Attribution (CC BY) license (<http://creativecommons.org/licenses/by/4.0/>).